2022 44th Annual International Conference of
the IEEE Engineering in Medicine & Biology Society (EMBC)
Scottish Event Campus, Glasgow, UK, July 11-15, 2022

2022 44th Annual International Conference of the IEEE Engineering in Medicine & Biology Society (EMBC) | 978-1-7281-2782-8/22/$31.00 ©2022 IEEE | DOI: 10.1109/EMBC48229.2022.9871419

3D+t feature-based descriptor for unsupervised flagellar human sperm beat classification

Haydee O. Hernández[1,2,4], Paul Hernández-Herrera[2,3], Fernando Montoya[2], Jimena Olveres[4], Hermes Bloomfield-Gadêlha[5], Alberto Darszon[6], Boris Escalante-Ramírez[4] and Gabriel Corkidi[2]

***Abstract*— Human spermatozoa must swim through the female reproductive tract, where they undergo a series of biochemical and biophysical reactions called capacitation, a necessary step to fertilize the egg. Capacitation promotes changes in the motility pattern. Historically, a two-dimensional analysis has been used to classify sperm motility and clinical fertilization studies. Nevertheless, in a natural environment sperm motility is three-dimensional (3D). Imaging flagella of freely swimming sperm is a difficult task due to their high beating frequency of up to 25 Hz. Very recent studies have described several sperm flagellum 3D beating features (curvature, torsion, asymmetries, etc.). However, up to date, the 3D motility pattern of hyperactivated spermatozoa has not been characterized. The main difficulty in classifying these patterns in 3D is the lack of a ground truth reference since differences in flagellar beat patterns are very difficult to assess visually. Moreover, only around 10-20% of induced to capacitate spermatozoa are truly capacitated, i.e., hyperactivated. We used an image acquisition system that can acquire, segment, and track spermatozoa flagella in 3D+t. In this work, we propose an original three-dimensional feature vector formed by ellipses describing the envelope of the 3D+t spatio-temporal flagellar sperm motility patterns. These features allowed compressing an unlabeled 3D+t dataset to separate hyperactivated cells from others (capacitated from non-capacitated cells) using unsupervised hierarchical clustering. Preliminary results show three main clusters of flagellar motility patterns. The first principal component of these 3D flagella measurements correlated with 2D OpenCASA head determinations as a first approach to validate the unsupervised classification, showing a reasonable correlation coefficient near to 0.7.**

***Clinical relevance*— The novelty of this work is defining a 3D+t feature-based descriptor consisting of a set of ellipses enveloping the flagellar motion of human sperm for its unsupervised classification. This is a new promising tool to determine the viability of human sperm to fertilize the egg.**

I. INTRODUCTION

Fertilization requires spermatozoa to swim through the female tract to reach the egg. During their journey, sperm undergoes a capacitation process involving important biochemical and biophysical changes necessary to fertilize the egg. Clinical analysis performed in two-dimensional images has shown that sperm induced to capacitate present different types of motility, notably the hyperactivated one. Hyperactivated motility in 2D is characterized by a high flagellar asymmetrical amplitude bend [1]. From millions of ejaculated spermatozoa, only an average of 10-20% are capacitated (able to fertilize), presenting hyperactivated motility [2]. Semen analysis is the first test indicated to determine the infertility of a couple, including the analysis of sperm morphology, concentration, motility, and semen viscosity. For three decades, the analysis of sperm motility has been performed by tracking the sperm heads in 2D images. Historically, this study was carried out by experts (physiologists or embryologists) based on their own judgement, making results inaccurate, subjective, and irreproducible [3,4]. Computer Assisted Semen Analysis (CASA) has become the reference analysis system since it uses quantitative parameters to classify sperm motility [4]. Recently, a significant effort has been made to automate and remove subjectivity in this type of analysis by applying machine learning and deep learning techniques to classify sperm motility and morphology [5-8]. However, most determinations have been based only on the sperm head trajectory and CASA parameters from 2D images, excluding flagellar movement. 3D imaging sperm flagella kinematics faces important computational problems such as acquisition, detection, segmentation, tracking, and classification [9]. In the last years, important contributions have arisen to solve part of these problems and to obtain information on single sperm in 3D, particularly the description of its flagella kinematics [9-13]. Nevertheless, the classification of 3D flagellar beating patterns of capacitated sperm remains an open research field.

Multiple methods to classify 3D dynamic patterns have been reported [14,15] however, the comparison between shapes varying over time is a complicated task, especially in motion recognition or video classification [16]. In this work, we propose an original dynamic motility descriptor consisting of a set of ellipses enveloping the flagella from which a set of features are derived. This descriptor feature-based vector allows compacting the flagellar beat information from the acquired 3D+t data of variable size (number of points per flagellum and acquisition time per sperm). Our experimental dataset consisted of 100 free-swimming sperm acquired in 3D with a system as described in [9], beating during 1 to 3 seconds. The set was composed of non-capacitated sperm (control) and sperm pharmacologically induced to capacitate, where a fraction may be hyperactivated. It is important to

[1]Posgrado en Ciencia e Ingeniería de la Computación, UNAM, Mexico City, Mexico
[2]Laboratorio de Imágenes y Visión por Computadora, Instituto de Biotecnología, UNAM, Cuernavaca, Mexico
[3]Laboratorio Nacional de Microscopía Avanzada, Instituto de Biotecnología, UNAM, Cuernavaca, Mexico
[4]Departamento de Procesamiento de Señales, Facultad de Ingeniería, UNAM, Mexico City, Mexico
[5]Department of Engineering Mathematics and Bristol Robotics Laboratory, University of Bristol, Bristol, UK
[6]Departamento de Genética del Desarrollo y Fisiología Molecular, Instituto de Biotecnología, UNAM, Mexico City, Mexico

emphasize that our dataset is unlabeled, it is not possible to identify visually the different beating patterns. Thanks to the proposed dynamic flagella descriptor, we were able to use hierarchical clustering, a simple unsupervised classification technique, to group non-capacitated sperm, from those, truly capacitated (hyperactivated), describing the shape and similarities between the samples to cluster into distinct types of beating.

II. Materials and Methods

A. Biological preparations

Human spermatozoa samples were obtained from healthy donors after a minimum abstinence of 48 hours. From the collected samples, a 1-hour swim-up protocol was performed to select the highly motile cells. Half of these cells were centrifuged during 5 minutes and resuspended at a concentration of 10^7 cells/ml in a non-capacitating solution. Capacitation was induced in the other half of the highly motile cells by resuspending them in a capacitation solution and incubating them for six hours.

B. Experimental set-up

The acquisition system includes an inverted Olympus IX71 microscope mounted on an optical table with a 60x water immersion objective with a $N.A. = 1.00$ oscillating on a piezoelectric device P-725. A servo-controller E-501 via a high current amplifier E-505 (hardware from Physik Instrumente, MA, USA) was used to control the piezoelectric device. The high-speed camera NAC Q1v with 8 Gigabyte RAM (recording up to 8000 images per second of 640 x 480 pixels for 3.5 seconds) is triggered by a TTL pulse from the servo-controller which is driven by a ramp signal from the E-506 function generator. The temperature of the spermatozoa samples was maintained with a thermal controller at $37°C$.

C. Dataset

Data were collected with the system described by Corkidi et al. [9] and the segmentation process to reconstruct the flagellum centerline as described by Hernández-Herrera et al. [11].
The dataset consisted of 100 human spermatozoa, from which 81 sperm underwent an *in-vitro* capacitation process (induced to capacitate) and 19 were non-capacitated. A fraction of 10-20% of sperm induced to capacitate is expected to be hyperactivated [2]. Given a sperm i from the dataset, the flagellum's centerline was tracked during $T-$times and described by N_T-points in 3D coordinates where $\{x^i_{tn}, y^i_{tn}, z^i_{tn}\}$ correspond to the *n-th* position of the flagellum's centerline at time point t for sperm i, $t \in 1, 2, ..., T$ and $n \in 1, 2, ..., N$. Due to the segmentation process, the number of detected flagella and points per single beat are different over time. Flagella were rotated and translated to align with the $x-$axis starting from the origin.

D. Ellipse fitting

Fig. 1 shows a reconstructed flagella aligned with $x-$axis. We define a flagelloid F^i_l for sperm i to be the orthogonally projected points in the interval $[l, l+1)$ (Fig. 2);

$$F^i_l = (y^i_{tn}, z^i_{tn}) | x^i_{tn} \in I_{l,l+1} \quad (1)$$

where $I_{l,l+1}$ are the cutting planes of the interval $[l, l+1), l \in \{0\mu m, 0.2\mu m, \ldots, 120\mu m\}$. Fig. 2 shows the fitting of an ellipse to the points belonging to the flagelloid (1), using the method of "Direct fit of least squares of ellipses" as described in [17]. Doing this for each flagelloid l, a set of transverse ellipses on the x-axis are obtained describing the motility shape of the sperm (Fig. 3). The interval size is equal to $0.2\mu m$, this value was determined experimentally in such a way that each interval contains approximately three points; ellipses are fitted only when the flagelloid has at least these number of points and these are no collinear, to prevent that $\epsilon \to 1$. From each ellipse we obtain four parameters:

- Semi-major axis (a)
- Semi-minor axis (b)
- Rotation angle of the ellipse (ϕ)
- Eccentricity (ϵ).

To describe the envelope of ellipse variations, we applied simple linear regression to the cumulative sum for a, b, and ϕ; in addition of the mean (μ) of a, b, and ϵ. Thus, having the feature-based vector with six components:

$$\begin{aligned}\mathbf{v} =& [slope(cumsum(a)), slope(cumsum(b)),\\ & slope(cumsum(\phi)), \mu(a), \mu(b), \mu(\epsilon)].\end{aligned}$$

We performed dimensionality reduction, applying Principal Component Analysis, to three principal components (more than 90% of the variance in the dataset). The dominant features for each principal component are: $\mu(b), \mu(\epsilon)$ and $slope(cumsum(\phi))$, respectively.

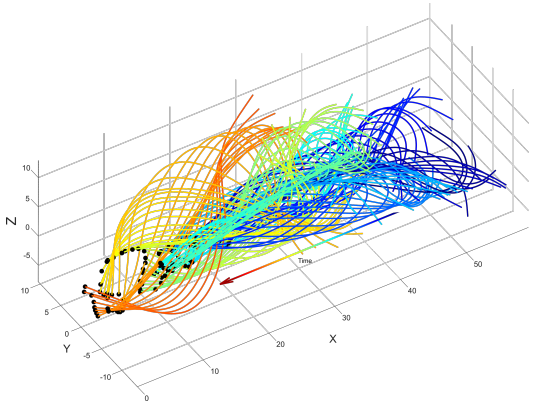

Fig. 1. Representation of the segmented and tracked spermatozoon. Data are aligned with x-axis, each line corresponds to a flagellum reconstruction at time t and the black dots represent the first point of the flagella at each time. The progression of swimming is from $+x \to 0$. The color scale represents the progression of the beat, the blue color is the initial flagella time advancing towards the red.

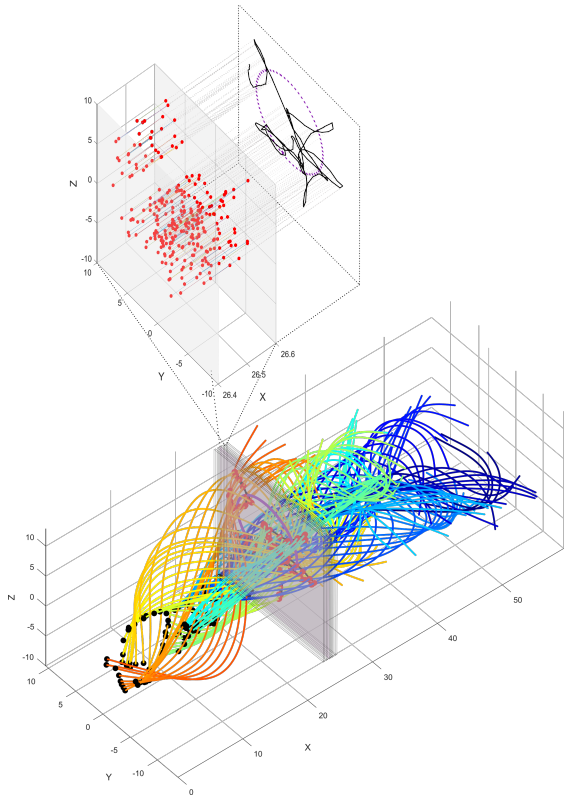

Fig. 2. Scheme to fit an ellipse to the flagelloid. The bottom subplot shows the representation of the segmented and tracked spermatozoon from Fig. 1; 10 from 298 gray planes (only for observation purposes) corresponding to 5 intervals ($0.2\mu m$ each) are shown. The upper subplot shows a zoom of a single $0.2\mu m$ selected interval, the red dots corresponding to the flagellum points within that interval. The right upper side shows the orthogonal projection of the red dots forming a flagelloid (black line) with its corresponding fitted ellipse (purple-dotted line).

E. Clustering

Our dataset contains non-capacitated sperm (control) and induced to capacitate sperm. Concerning the latter, we know that a small fraction should be hyperactivated (10 to 20%). Since hyperactivated sperm are not labeled, we do not have a priori information on the number of clusters in our database and our dataset is small, thus we applied agglomerative hierarchical clustering, since it allows to have a visual hint of how the groups relate to each other. Hierarchical clustering does not require input parameters for clustering, has low sensitivity to outliers and does not require knowing the number of clusters. We calculate the Euclidean distance between each pair of sperm for the three principal components to find the dissimilarity. The proximity between objects was carried out with an average linkage, using 'distance' as the criterion for defining 3-clusters. The dendrogram allows us to visually determine how many main groups there were. We have defined three clusters, control cells (non-capacitated), hyperactivated cells (truly capacitated) and as mentioned by Mortimer et al. [4] and de Lamirande et al. [18], spermatozoa present a transitional state conforming the third cluster.

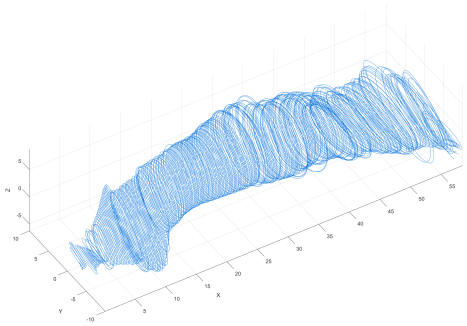

Fig. 3. Ellipse envelope for a spermatozoon. Each ellipse corresponds to an interval along the flagellum.

III. Preliminary Results

Fig. 4 shows the dissimilarity matrix of the Euclidean distance between each pair of spermatozoa which shows how close they are according to their feature-based descriptor. The diagonal of the matrix is completely black since the distance of a feature-based descriptor against itself is 0 (high similarity), while pairs of feature-based descriptors with higher distances are represented with white (low similarity). Cluster 1 (green lines) contains the non-capacitated cells and a subset of the induced to capacitate (not hiperactivated) sperm. Cluster 2 (red lines) is constituted by sperm whose fitted ellipses had a semi-major axis with a value larger than ($a > 5\mu m$) compared with cluster 1, in addition $\epsilon \rightarrow 1$ (see Discussion for the interpretation). Cluster 3 (blue lines) contains those spermatozoa that, like cluster 2, present the semi-major axis with a value larger than cluster 1, however the eccentricity tends to 0.7.

Hierarchical clustering formed three main groups: non-capacitated, transitional and hyperactivated sperm (Fig. 5). The non-capacitated motility group corresponds to cluster 1, with the complete set of non-capacitated sperm and a subset of induced to capacitate sperm. Sperm with a transitional motility correspond to cluster 3 and hyperactivated cells to cluster 2. The hierarchical clustering has a cophenetic correlation coefficient of 0.7764, which is an acceptable value implying that the original distances between the samples are preserved. Although the clustering method presented outliers, these were less than 5% and since we used an average linkage, it is not affected by these outliers.

We used OpenCASA as a preliminary approach to validate our results, with the sperm head trajectory (ALH, Amplitude of Lateral Head Displacement). ALH (also referred as 'head yawing'), is the maximum head displacement from the average trajectory tracked. This measurement refers to the vigor and amplitude of the flagellar beat. It has been observed that high values of ALH correlate with hyperactivated motility. OpenCASA is an open-source software that computes CASA measurements in 2D images [19]. We projected the 3D sperm head coordinates in $x - y$ plane to obtain the head trajectory. The correlation between the ALH value and the first component of principal component analysis showed a reasonable correlation coefficient near 0.7.

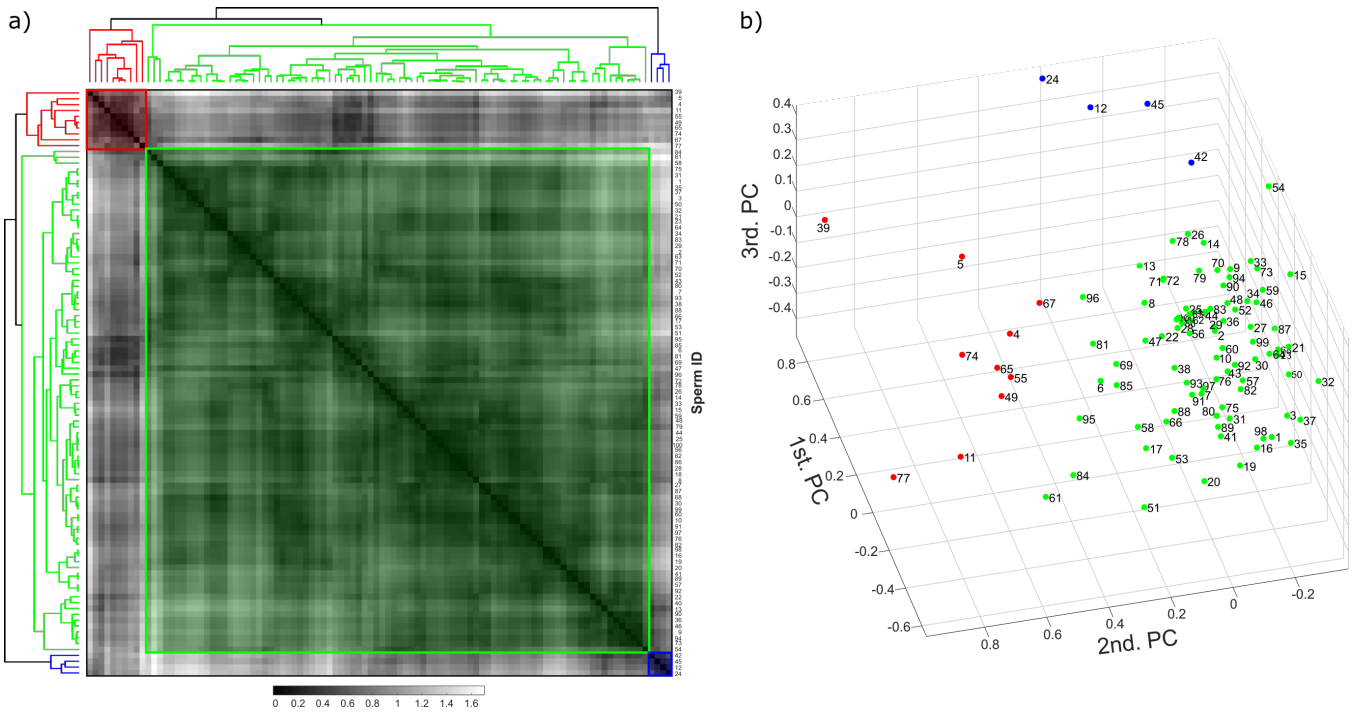

Fig. 4. a) Dissimilarity matrix from the Euclidean distance of the three principal components between each pair of sperms, pixel intensity corresponds to the distance value. Sperm IDs correspond to the number of the experiment, where 1-81 correspond to sperm induced to capacitate and 82-100 are the non-capacitated ones. The dendrogram shows the hierarchical clustering with average linkage; green lines correspond to cluster 1 (4, 5, 11, 39, 49, 55, 65, 67, 74 and 77), red lines to cluster 2 (12, 24, 42 and 45) and blue lines to cluster 3. b) Clustering of flagellar motility for the dataset. The labels of the dots correspond to the number of the experiment. Green dots correspond to cluster 1, red dots to cluster 2 and blue dots to cluster 3.

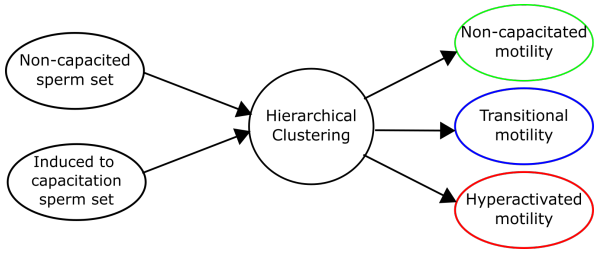

Fig. 5. Clustering diagram resulting from the proposed method. The input data are non-capacited and induced to capacitate spermatozoa. When clustering is applied, three main groups of motility patterns are obtained: non-capacitated, transitional and hyperactivated.

IV. Conclusions and Discussion

The novelty of the feature-based vector that we propose in this work encompasses the flagella beating pattern of sperm. Thanks to the performance of these features to describe the flagella dynamics, it was possible to use a simple unsupervised classification technique to group non-capacitated sperm, from those truly capacitated (hyperactivated). An ellipse eccentricity close to 1, means that the ellipse is elongated (corresponding to an asymmetric beating pattern trend), while when eccentricity tends to 0 it is more circular (symmetric beating pattern trend). It is known that the beating pattern of non-capacitated spermatozoa is more symmetric than that for hyperactivated ones [1]. Given the previous considerations, the first cluster (Fig. 4a, green lines) corresponds to the motility pattern of non-capacitated sperm (control sperm + those induced that failed-to-capacitate) given that the semi-major axis of the fitted ellipses are smaller compared to the other clusters, in addition, the mean eccentricity is smaller, tending to 0.5. Failed-to-capacitate spermatozoa are those sperms that were induced to capacitate but exhibit swimming behavior similar to those observed from the control sperm. The trend of the spermatozoa found in this cluster shows motility characteristics that, according to the literature, are associated with spermatozoa that were non-capacitated, meaning that the beat pattern of this cluster is more symmetrical and of smaller amplitude compared to the other groups. We consider the third cluster (Fig. 4a, blue lines) as being a transitional beating pattern from non-capacitated to capacitated (hyperactivated) spermatozoa; since the amplitude of the semi-major axis increases relative to cluster 1 and the average eccentricity also increases, tending to 0.7, i.e., the flagellar beat has an increasing amplitude and sperm begin to display an asymmetrical beat. We infer that the second cluster (Fig. 4a, red lines) corresponds to the hyperactivated beating pattern, since its average eccentricity tends to 1, with a larger amplitude compared to cluster 1, implying an asymmetric motility pattern, as mentioned previously. Furthermore, as expected, ≈12% of the induced to capacitate spermatozoa belong to this cluster as mentioned in [2]. It is important to point out that the whole set of non-capacitated sperm was correctly classified in the green cluster together with the failed-to-capacitate from the induced group. Although this task could be thought of as a binary classifi-

cation, the motility exhibited by sperm in a population is heterogeneous, and a sperm induced to capacitation should exhibit a change in the flagellar beat that is not instantaneous. Therefore, the classification cannot be reduced to only two classes, so adding a third class (transitional) of motility allows us to distinguish those spermatozoa that we suppose are undergoing a change in their flagellar beat at the time the images were acquired.

As we mentioned before, no ground-truth exists for 3D classification purposes, thus the correlation coefficient of the first principal component with the ALH value for all spermatozoa was a first approach to validate the unsupervised classification results. Although some experiments agree with their ALH value and clustering, the comparison with CASA values is limited since it is based on the head movement, while in this work, we are measuring the 3D flagellar dynamics. Further analysis is required to establish a truth reference in order to have a better way to measure the performance of the proposed method. Actually, we are increasing the number of experiments to balance the database with one hundred sperm per condition to give a more robust proof of the validity of the proposed method; these results will be presented in an upcoming work. Our findings are promising given that flagella hyperactivation has never been described in 3D. They will contribute to define the parameters for the classification of the hyperactivated motility pattern in 3D.

COMPLIANCE WITH ETHICAL STANDARDS

This work was approved by the Bioethics Committee permit for project IN200919. Signed written informed consent forms were signed by all healthy donors.

ACKNOWLEDGMENT

This work was supported by UNAM (PAPIITs IN200919, TA101121, IV100420, IN105222) and CONACyT (CVU 700563).

REFERENCES

[1] Dagmar Waberski, Susan S Suarez, and Heiko Henning, "Assessment of sperm motility in livestock: perspectives based on sperm swimming conditions in vivo," *Animal Reproduction Science*, p. 106849, 2021.

[2] Susan S Suarez, "Control of hyperactivation in sperm," *Human reproduction update*, vol. 14, no. 6, pp. 647–657, 2008.

[3] Daznia Bompart, Almudena García-Molina, Anthony Valverde, Carina Caldeira, Jesús Yániz, Manuel Núñez de Murga, and Carles Soler, "Casa-mot technology: how results are affected by the frame rate and counting chamber," *Reproduction, Fertility and Development*, vol. 30, no. 6, pp. 810–819, 2018.

[4] Sharon T Mortimer, Gerhard van der Horst, and David Mortimer, "The future of computer-aided sperm analysis," *Asian journal of andrology*, vol. 17, no. 4, pp. 545, 2015.

[5] Soroush Javadi and Seyed Abolghasem Mirroshandel, "A novel deep learning method for automatic assessment of human sperm images," *Computers in biology and medicine*, vol. 109, pp. 182–194, 2019.

[6] Pedro Ângelo Pereira da Silva, *Supervised and unsupervised spermatozoa detection, classification and tracking in imaging data*, Ph.D. thesis, 2011.

[7] Summer G Goodson, Sarah White, Alicia M Stevans, Sanjana Bhat, Chia-Yu Kao, Scott Jaworski, Tamara R Marlowe, Martin Kohlmeier, Leonard McMillan, Steven H Zeisel, et al., "Casanova: a multiclass support vector machine model for the classification of human sperm motility patterns," *Biology of reproduction*, vol. 97, no. 5, pp. 698–708, 2017.

[8] Jason Riordon, Christopher McCallum, and David Sinton, "Deep learning for the classification of human sperm," *Computers in biology and medicine*, vol. 111, pp. 103342, 2019.

[9] G Corkidi, B Taboada, CD Wood, A Guerrero, and A Darszon, "Tracking sperm in three-dimensions," *Biochemical and biophysical research communications*, vol. 373, no. 1, pp. 125–129, 2008.

[10] G Corkidi, F Montoya, P Hernández-Herrera, WA Ríos-Herrera, MF Müller, CL Treviño, and A Darszon, "Are there intracellular ca2+ oscillations correlated with flagellar beating in human sperm? a three vs. two-dimensional analysis," *MHR: Basic science of reproductive medicine*, vol. 23, no. 9, pp. 583–593, 2017.

[11] Paul Hernandez-Herrera, Fernando Montoya, Juan Manuel Rendón-Mancha, Alberto Darszon, and Gabriel Corkidi, "3-d+t human sperm flagellum tracing in low snr fluorescence images," *IEEE transactions on medical imaging*, vol. 37, no. 10, pp. 2236–2247, 2018.

[12] Hermes Gadêlha, Paul Hernández-Herrera, Fernando Montoya, Alberto Darszon, and Gabriel Corkidi, "Human sperm uses asymmetric and anisotropic flagellar controls to regulate swimming symmetry and cell steering," *Science advances*, vol. 6, no. 31, pp. eaba5168, 2020.

[13] A Gong, Sebastian Rode, G Gompper, Ulrich Benjamin Kaupp, J Elgeti, BM Friedrich, and Luis Alvarez, "Reconstruction of the three-dimensional beat pattern underlying swimming behaviors of sperm," *The European Physical Journal E*, vol. 44, no. 7, pp. 1–12, 2021.

[14] Antonios Danelakis, Theoharis Theoharis, Ioannis Pratikakis, and Panagiotis Perakis, "An effective methodology for dynamic 3d facial expression retrieval," *Pattern Recognition*, vol. 52, pp. 174–185, 2016.

[15] Marcel Körtgen, Gil-Joo Park, Marcin Novotni, and Reinhard Klein, "3d shape matching with 3d shape contexts," in *The 7th central European seminar on computer graphics*. Citeseer, 2003, vol. 3, pp. 5–17.

[16] Peng Huang, Jonathan Starck, and Adrian Hilton, "Temporal 3d shape matching," in *4th European Conference on Visual Media Production*. IET, 2007, pp. 1–10.

[17] Eliseo Stefano Maini, "Enhanced direct least square fitting of ellipses," *International Journal of Pattern Recognition and Artificial Intelligence*, vol. 20, no. 06, pp. 939–953, 2006.

[18] Eve de Lamirande, Pierre Leclerc, and C Gagnon, "Capacitation as a regulatory event that primes spermatozoa for the acrosome reaction and fertilization," *Molecular human reproduction*, vol. 3, pp. 175–94, 04 1997.

[19] Carlos Alquézar-Baeta, Silvia Gimeno-Martos, Sara Miguel-Jiménez, Pilar Santolaria, Jesús Yániz, Inmaculada Palacín, Adriana Casao, José Álvaro Cebrián-Pérez, Teresa Muiño-Blanco, and Rosaura Pérez-Pé, "Opencasa: A new open-source and scalable tool for sperm quality analysis," *PLoS computational biology*, vol. 15, no. 1, pp. e1006691, 2019.